Core-level photoemission measurements of valence-band offsets in highly strained heterojunctions: Si-Ge system

G. P. Schwartz, M. S. Hybertsen, J. Bevk, R. G. Nuzzo, J. P. Mannaerts, and G. J. Gualtieri
AT&T Bell Laboratories, Murray Hill, New Jersey 07974
(Received 21 July 1988)

The binding-energy separation between the Si 2*p* and Ge 3*d* core levels has been measured on pseudomorphically strained heterojunctions consisting of Si on Ge(100) and Ge on Si(100) using x-ray photoemission. Analysis shows that the core-level binding energies referenced to the top of the valence band depend explicitly on strain. As a consequence, the use of core-level data from unstrained materials is inappropriate for determining valence-band offsets in highly strained heterojunctions. Our data have been supplemented by calculations of the relative core–valence-band deformation potentials. These results, together with the calculated uniaxial component of the valence-band splitting and the measured $E_{\mathrm{Si}\,2p}-E_{\mathrm{Ge}\,3d}$ energy difference on strained heterojunctions, allow us to estimate valence-band offsets of 0.74 ± 0.13 and 0.17 ± 0.13 eV for Ge on Si(100) and Si on Ge(100), respectively.

I. INTRODUCTION

The substantial reevaluation of heterojunction band offsets which has occurred during the last decade highlights the formidable experimental and theoretical difficulties encountered in the field. At the present time, the best characterized heterojunction systems tend to be those which are lattice matched, and within this context, core-level photoemission has emerged as one of the primary measurement techniques.[1,2] Materials of interest today, however, often include strained-layer structures. In such systems, strain introduces both a shift and splitting of the core and valence bands, with the resulting band discontinuities depending explicitly on which material is under strain. In principle, the core levels referenced to the top of their strain-split valence bands are no longer equal to those in unstrained materials, as was recently pointed out by Tersoff and Van de Walle.[3] Nevertheless, a large body of photoemission data exists in the literature purporting to measure valence-band offsets in highly strained, lattice-mismatched heterojunctions in which unstrained reference core levels were utilized in the data analysis. Such an approach will yield the correct valence-band offset only in the unlikely case that the strained core level happens to track the top of the valence band. The present study has examined a system with a high degree of in-plane biaxial strain achieved by pseudomorphic epitaxy. It is explicitly demonstrated that the relevant strained core levels do not track the top of the valence band. We further demonstrate the manner in which the heterojunction core-level measurements must be supplemented in order to obtain meaningful valence-band discontinuities. At issue is the correct use of photoemission data in determining valence-band offsets in highly strained heterojunctions.

The Si/Ge system was chosen for analysis for several reasons. First, it displays a large room-temperature lattice mismatch (4%). Second, the growth characteristics and critical layer thicknesses necessary to achieve pseudomorphic epitaxy are known.[4] Third, theoretical calculations of the valence-band offsets are available.[5] Finally, critically selected experimental data[6] indicates that the calculations provide an accurate assessment of the relevant band offsets. Heterojunction samples of Si on Ge(100) and the reverse sequence were grown by molecular-beam epitaxy. The strain was verified by Raman measurements. The binding-energy separation between the Si 2*p* and Ge 3*d* core levels was measured for both growth sequences, and the resulting data analyzed to show that the core-level energy referenced to the top of the valence band depends explicitly on the strain. The heterojunction core-level measurements were supplemented by core–valence-band deformation-potential calculations which allowed us to extract the valence-band offsets. For Si on Ge(100) we obtained a valence-band offset of 0.17 ± 0.13 eV. For the reverse sequence of Ge on Si(100) the offset is 0.74 ± 0.13 eV.

II. EXPERIMENT AND RESULTS

A. Heterojunction growth

Following previously described growth practices,[4] six monolayers (~ 8.7 Å including tetragonal distortion) of Ge were grown epitaxially on a Si(100) substrate and capped with 12 monolayers of Si (~ 16.3 Å). The cap was necessary to avoid oxidation of the Ge layer which would have altered its strain and obviated any meaningful comparison with theory. The Si cap, like the substrate, is nominally unstrained under pseudomorphic growth conditions. The term "nominally unstrained" has been used because some oxidation of the cap inevitably occurs during sample transfer to the photoemission instrument. Stress generated by differences in the cap-oxide thermal expansion coefficients can be neglected since the oxidation occurs at room temperature. Any epitaxy-derived stress which is generated should be

 ©1989 The American Physical Society

roughly partitioned between the oxide and substrate according to the ratio of the oxide thickness to the composite (substrate-film-cap) thickness. Since this ratio is $\sim 10^{-6}$, the cap should remain unstrained. For the reverse heterostructure, $\sim$2000 Å of Ge was grown on GaAs(100), followed by six monolayers of Si ($\sim$7.6 Å including tetragonal distortion) and then 12 monolayers of a Ge cap. The growth temperatures were $\sim$450 °C [infrared (ir) pyrometer].

B. Raman scattering

Shifts in the optic-mode phonon frequencies between the strained layers in the heterojunction samples and unstrained bulk wafers were measured using Raman scattering. Spectra were collected on a 1-m double monochromator with holographic gratings using standard pulse counting electronics. The excitation source was several hundred milliwatts of 5145-Å radiation from an Ar^+ laser polarized in the scattering plane and incident on the sample at Brewster's angle. The scattering geometry was $z(x,y)\bar{z}$, where x, y, and z denote the crystalline axes $x\|[010]$, $y\|[001]$, and $z\|[100]$. This scattering configuration selects out the singlet optic phonon in a thin film with biaxial stress in the x-y plane.[7] The data were all taken at room temperature in an evacuated cell.

Figure 1 shows the Raman spectra for each type of heterojunction structure. Relative to unstrained material, the optic-mode frequency of the strained Si layer decreases by 45 cm^{-1} whereas that of strained Ge increases by $\sim$4 cm^{-1}. The peak structures labeled by IFB refer to interfacial Ge—Si bonding and are not of importance to the present discussion. Since comparison with theory requires an accurate assessment of the strain actually present in the samples, we will present the Raman analysis in detail.

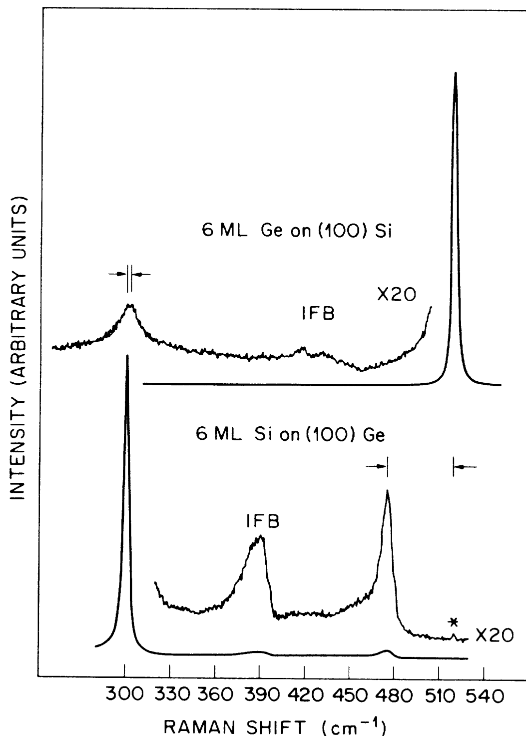

FIG. 1. Raman spectra illustrating the optic-phonon shifts observed for six monolayers of Ge on Si(100) and the reverse sequence. IFB represents peaks associated with Ge—Si interfacial bonding. The asterisk denotes a laser plasma line at 520.3 cm^{-1}.

There are two components contributing to the optic-mode shift: strain and quantum confinement. Strain splits the threefold degenerate optic modes into a singlet Ω_s and doublet Ω_d under a tetragonal distortion. The frequency shift of the singlet mode relative to the unstrained frequency $\delta\omega_s \equiv (\Omega_s - \omega_0)$ can be written as[8]

$$\delta\omega_s = \omega_0 \left[\tilde{K}_{12} + \tilde{K}_{11} \left[\frac{S_{12}}{S_{11}+S_{12}} \right] \right] \epsilon_{xx} , \quad (1)$$

where ω_0 is the unstrained frequency, $\tilde{K}_{ij}$ are dimensionless (normalized in units of ω_0) phonon deformation-potential matrix elements, S_{ij} are elastic compliances, and $\epsilon_{xx} = \epsilon_{yy} \equiv (a^s - a^f)/a^f$, where a^f and a^s are the film and substrate lattice constants. For the room-temperature Si and Ge lattice constants we have used 5.430 95 and 5.646 13 Å, respectively. The other parameters entering the calculation are tabulated in Table I from data in Refs. 8 and 9. The strain-induced component of the frequency shifts are -30.1 cm^{-1} for Si (tension) and $+15.8$ cm^{-1} for Ge (compression).

The remainder of the observed shift results from phonon quantum confinement. Based on a nearest-neighbor linear-chain model,[10] confinement in a six monolayer Si film should reduce the optic frequency by $\sim$12 cm^{-1}. The combination of strain and confinement suggests a downshift $\delta\omega_s$ around 42 cm^{-1}, in reasonable agreement with the observed value of 45 cm^{-1}. Similarly for Ge one would estimate a net positive shift $\delta\omega_s \sim 15.8 - 12 \sim 3.8$ cm^{-1}. In this case the agreement may be fortuitous because a Si acoustic mode overlaps the Ge optic mode throughout the latter's entire frequency range, thereby making propagating rather than confined solutions to the elastic wave equation possible.[11] Lattice-dynamics calculations in Ge/Si superlattices[12] support the concept of pseudoconfinement of the Ge optic phonons, however, based on an analysis of the displacement amplitudes. Despite this ambiguity, our current estimate for the frequency shift is not at variance with the Ge layer being fully strained.

C. X-ray photoemission

Core-level spectra were acquired with a Kratos Analytical Instruments XSAM-800 electron spectrometer. The data were acquired in the fixed analyzer transmission mode using Al $K\alpha$ excitation with an instrumental resolution $\sim$1.1 eV. In the photoemission experiments the core-level separation between the Si $2p$ and Ge $3d$ peaks was measured on the heterojunction samples described previously. The data were fitted in both cases to two spin-orbit-split components of equal width whose integrated areas were constrained to scale as $2J+1$. The spin-orbit splittings utilized in the fits were 0.61 and 0.54

TABLE I. Parameters for calculating the strain component of optic-mode shifts.

	ω_0 (cm^{-1})	$\tilde{K}_{11}$	$\tilde{K}_{12}$	$10^{-2}\epsilon_{xx}$	$S_{12}/(S_{11}+S_{12})$	$\delta\omega_s$ (cm^{-1})
Si	520.1	−1.40	−2.00	+3.962	−0.3857	−30.1
Ge	300.6	−1.47	−1.93	−3.811	−0.3754	+15.8

eV for the Si 2p and Ge 3d levels, respectively. Typical spectra for Si on Ge(100) are shown in Fig. 2. Since the strain is biaxial, there is a tetragonal as well as a hydrostatic component which, in principle, will split the core levels. Calculated estimates indicated that this splitting was small compared to the spin-orbit term and as a result it was neglected in the fits. An average binding energy weighted by the $2J+1$ intensity factors was calculated from the fits because the instrumental resolution was insufficient to resolve the individual components. This weighted average will be denoted by a bar ($\bar{E}_{\mathrm{Si}\ 2p}$, $\bar{E}_{\mathrm{Ge}\ 3d}$), so that in all subsequent discussion $\Delta E_{1,2} \equiv \bar{E}_{\mathrm{Si}\ 2p} - \bar{E}_{\mathrm{Ge}\ 3d}$, where the subscript order 1,2 denotes Si on Ge(100), and 2,1 Ge on Si(100).

Two samples of each heterostructure type were analyzed. For the case where six monolayers of Si were grown on Ge(100), the measured $\bar{E}_{\mathrm{Si}\ 2p} - \bar{E}_{\mathrm{Ge}\ 3d}$ core-level differences ($\Delta E_{1,2}$) were 70.18 and 70.06 eV. Both of these samples were grown at a substrate temperature of $\sim$450 °C. For Ge on Si(100), the first sample was grown at $\sim$450 °C, whereas the second sample was grown around 220 °C and then annealed at $\sim$500 °C for 10 min *in situ* after the Si cap was grown. For these latter two samples $\Delta E_{2,1} = 69.94$ and 69.87 eV. Since the strain levels in each heterojunction grouping were indistinguishable in the Raman spectra, we will use the averages $\Delta E_{1,2} = 70.12$ eV and $\Delta E_{2,1} = 69.90$ eV in the remaining discussion. The estimated uncertainty in these figures is ± 0.10 eV.

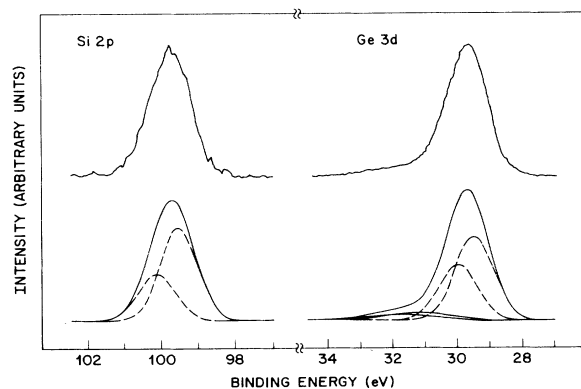

FIG. 2. Representative Si 2p and Ge 3d core-level spectra for the sample with six monolayers of Si on Ge(100), capped by 12 monolayers of Ge. The top panel shows the raw data; the lower panel shows the computed fit (solid) and its decomposition into spin-orbit split doublets (dashed). For the Ge 3d, oxidation of the cap contributes a broad shoulder 2–3 eV to higher binding energies above the unoxidized core levels (dashed).

III. DISCUSSION

In this section we wish to examine the issue related to utilizing unstrained core-level data in extracting valence-band offsets, and to demonstrate the supplementary calculations necessary for correct analysis. The photoemission technique consists of growing a thin heterojunction and recording the core-level separation, $\Delta E_{1,2}$, as shown in the energy-band diagram of Fig. 3. The heterojunction measurement must be supplemented by independent measurements of the individual core levels E_1 and E_2 properly referenced to their respective valence-band edges. In nearly lattice-matched systems which are essentially strain free, E_1 and E_2 can be taken from data on pure bulk materials. The valence-band offset ΔE_v follows from knowledge of E_1, E_2, and $\Delta E_{1,2}$.

In a strained heterojunction, the core-level separation measurement is performed similar to the unstrained case, however, the individual core levels E_1 and E_2 necessary to obtain the valence-band offset must be referenced to the top of their strain-split valence bands. The salient feature to note is that the strained binding-energy values need not be equal to those derived from unstrained bulk data. Only in the fortuitous situation where the core levels track the top of the valence band as a function of

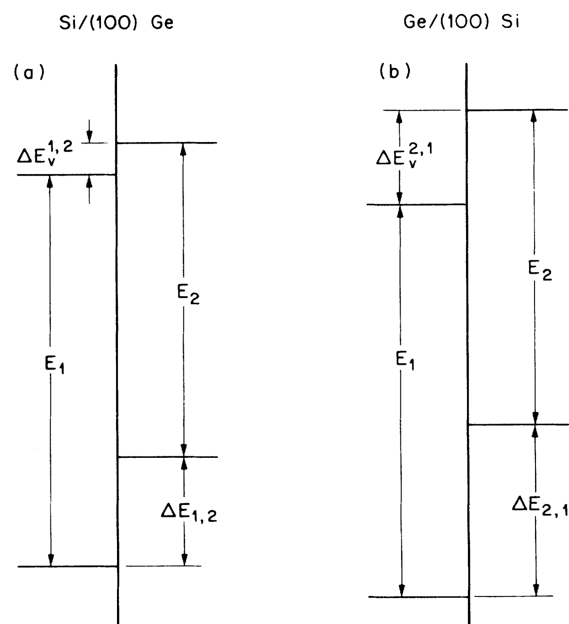

FIG. 3. Schematic energy-band diagrams for (a) Si on Ge(100) and (b) Ge on Si(100) assuming that the core levels track the top of the strain-split valence bands. The energy axes are not drawn to scale in Figs. 3–6.

strain can such data be used. In this context, tracking the top of the valence band means E_1(strain free)$=E_1$ (strain) and similarly for E_2.

A test of whether the core levels track the strain-split valence bands can be made based on prior knowledge of the band offsets in the Si/Ge system. The calculations of Van de Walle and Martin[5] for the (100) orientation of Si/Ge heterojunctions predicted band offsets of 0.84 and 0.31 eV, respectively, for Ge on Si and Si on Ge. Assuming that E_1 and E_2 do track their respective valence-band edges, one can write the following equations based on Fig. 3:

$$\Delta E_v^{2,1}+E_1=E_2+\Delta E_{2,1}\ , \tag{2a}$$

$$\Delta E_v^{1,2}+E_1=E_2+\Delta E_{1,2}\ . \tag{2b}$$

Combining (2a) and (2b) then gives the result $(\Delta E_v^{2,1}-\Delta E_v^{1,2})=(\Delta E_{2,1}-\Delta E_{1,2})$. The accuracy with which this expression can be evaluated depends on the precision with which one can measure the separation of two core levels on a given heterojunction sample, and does not depend on establishing accurately referenced binding energies for E_1 and E_2 since these parameters both drop out of the expression. The left-hand side represents the difference in valence-band offsets for Ge/Si(100) minus Si/Ge(100), which from theory is $0.84-0.31=0.53$ eV. The right-hand side is the difference in the $\bar{E}_{\mathrm{Si}\,2p}-\bar{E}_{\mathrm{Ge}\,3d}$ core-level separations measured on two heterojunction samples grown in reverse sequence relative to one another. From our data, $(\Delta E_{2,1}-\Delta E_{1,2})=69.90-70.12=-0.22$ eV. If we assume 0.10-eV error in each measurement and take the errors to add in quadrature, the uncertainty in the measurements would be ± 0.14 eV. It is more difficult to estimate the uncertainty in the theoretical calculation, but it should be borne in mind that since we are dealing with the difference in two valence-band offsets, the absolute accuracy of the individual band offsets is not the principle issue. Comparison with a recent experimental study suggests that the value of 530 meV is probably correct to 10–15%. These experimental measurements are from the photoemission study of Ni, Knall, and Hansson[6] on Si/(Si,Ge) heterojunctions. A critical aspect of their study is that their alloy reference core levels were taken on samples with the same degree of strain found in their undoped heterojunction structures. (Reference 6 should be consulted for additional details.) For $Si_{0.74}Ge_{0.26}$ and $Si_{0.52}Ge_{0.48}$ alloys grown pseudomorphically on Si(100) they obtain agreement with theory within some 10%. A comparable error in the 530-meV figure would be insignificant compared to the measured deviation. It is clear that in the Si/Ge system, the core levels do not track the top of their respective valence bands when the materials are strained.

We now discuss the relevance of our heterojunction core-level measurements for extracting valence-band offsets for both Ge on Si(100) and the corresponding reverse sequence. The biaxial strain associated with pseudomorphic epitaxy can be decomposed into hydrostatic (h) and uniaxial (u) components. $\Delta E_{1,2}$ and $\Delta E_{2,1}$ are the measured $\bar{E}_{\mathrm{Si}\,2p}-\bar{E}_{\mathrm{Ge}\,3d}$ core-level separations on the heterojunction samples. The quantities E_1 and E_2 can be obtained from the literature from high-resolution measurements on bulk materials. For the Ge 3d levels measured relative to the unstrained valence-band edge we used the (110) data of Kraut *et al.*,[13] $\bar{E}_{\mathrm{Ge}\,3d}=29.57$ eV. For Si, the $2p_{1/2}$ and $2p_{3/2}$ peaks have been scaled from Fig. 1(b) of Ref. 14 and corrected for $\varepsilon_F-\varepsilon_v=0.34$ eV for Si(100)-(2×1) to yield $\bar{E}_{\mathrm{Si}\,2p}=99.01$ eV. The quantities $\Delta E_{2,1}$ and $\Delta E_{1,2}$ were experimentally measured and values of 69.90 eV [Ge/Si(100)] and 70.12 eV [Si/Ge(100)] were obtained.

From the previous discussion it is clear that the cores do not track the top of the strain-split valence band. In the work of Ni, Knall, and Hansson,[6] the core levels were measured on strained reference samples relative to the top of the valence band by doping the materials p^+ to make the Fermi level coincide with the valence-band energies (VBE), and as a consequence, they obtained the strained reference core levels directly. Since our growth system does not presently incorporate doping sources, we must proceed by an alternate route in order to estimate the valence-band offsets. In the present case, the relative deformation potential for the core-level states with respect to the centroid of the valence-band edge states has been calculated. The uniaxial component of the distortion splits the valence-band degeneracy as well as the core level, but does not shift the centroid. The energy difference between the centroid of the valence-band edge and the core level is only influenced by the hydrostatic component. The latter is explicitly considered here. The calculation of the hydrostatic part of the relative deformation potential is based on comparing the core-level to valence-band edge separation in unstrained and strained bulk materials.

The calculations were carried out using the linear muffin-tin-orbital (LMTO) method with the atomic spheres approximation including the combined correction terms[15] and the local-density approximation (LDA).[16] The calculations were fully self-consistent. Details of the LMTO approach and explanations of terminology can be found in Ref. 15. Empty spheres were included in the standard fashion for tetrahedrally coordinated semiconductors.[17] The results reported here are based on fully relaxing the core level involved, e.g., Si 2p or Ge 3d. These core levels are handled in a lower-energy panel. The adequacy of this approach using $\kappa=0$ structure constants for the core levels was extensively tested. In particular, these core energies computed from the LMTO secular matrix agree quite well with eigenvalues obtained using free-atom boundary conditions with the same potential. Also, the final self-consistent valence-band structure agrees well with that obtained using the frozen core approximation. Finally, the relative hydrostatic deformation potentials for the X- and L-derived conduction-band minima agree within a few tenths of an eV with those calculated by Van de Walle and Martin.[5]

The results for the volume changes appropriate to perfect epitaxy in each case are as follows:

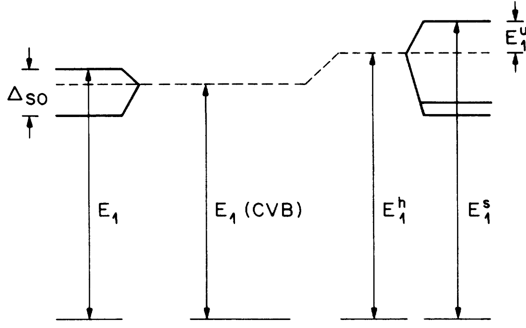

FIG. 4. Relation between the core levels measured on strain-free substrates relative to the top of the valence-band edge and their values referenced to the centroid of the valence-band edge states under strain. A similar diagram applies to the E_2 core level.

$$(E_{\mathrm{CVB}}-E_{\mathrm{Si}\ 2p})^h-(E_{\mathrm{CVB}}-E_{\mathrm{Si}\ 2p})^0=0.22\ \mathrm{eV}\ \text{for Si}\ ,$$

$$(E_{\mathrm{CVB}}-E_{\mathrm{Ge}\ 3d})^h-(E_{\mathrm{CVB}}-E_{\mathrm{Ge}\ 3d})^0=0.08\ \mathrm{eV}\ \text{for Ge}\ ,$$

where CVB designates the centroid of the valence-band edge levels, and the superscripts h and 0 denote hydrostatic and strain-free, respectively. Note that Si is under tension while Ge is compressed. Although the absolute values of the core levels are not necessarily accurate within the context of an LDA calculation, the differences calculated here are expected to be, in analogy with the deformation potentials associated with valence-band states. It is interesting to note that the $E_{\mathrm{Ge}\ 3d}-E_{\mathrm{CVB}}$ difference increases with pressure while the $E_{\mathrm{Si}\ 2p}-E_{\mathrm{CVB}}$ difference decreases. The former can be understood since the energy of p-like states always rises faster than that of d-like states with pressure. The Ge $3d$ states are sufficiently shallow in energy for this argument to be applicable. The case of the Si $2p$ states is rather different. The binding energy is sufficiently large that the radial extent of the wave functions is considerably less than for the valence-band states. Here, the change in the Si $2p$ core level closely follows the change in the potential near the site of the core. The sign of the change with pressure follows from the positive Madelung potential on a given site due to the surrounding charges (naturally the other Si spheres and the "empty" spheres in the LMTO method).

Because the unstrained reference core levels have been measured relative to the top of the valence band rather than to its centroid, one further correction is necessary as outlined in Fig. 4. For primarily p-like valence bands, we obtain the core-level binding energy referenced to the

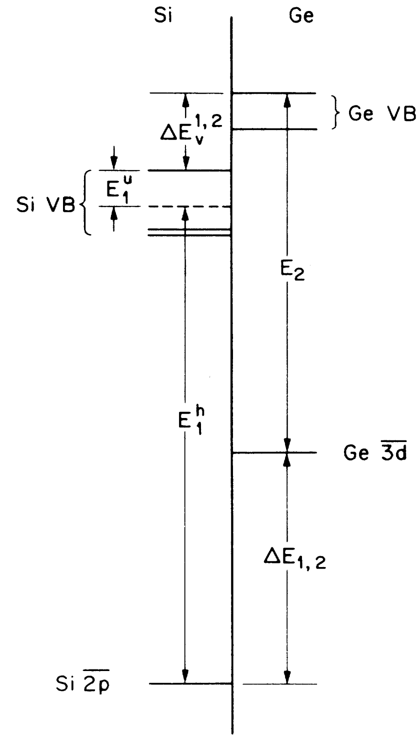

FIG. 5. Schematic energy-band diagram for Ge pseudomorphically strained to match the in-plane lattice constant on Si(100). The notation is delineated in the text, and Table III contains a compilation of the appropriate parameter values.

centroid of the valence band as $E_1(\mathrm{CVB})=E_1-\frac{1}{3}\Delta_{\mathrm{s.o.}}$, where $\Delta_{\mathrm{s.o.}}$ is the valence-band spin-orbit splitting. For Si and Ge we have used $\Delta_{\mathrm{s.o.}}=44$ and 282 meV, respectively. The hydrostatic contribution calculated using the LMTO method is then added to $E_1(\mathrm{CVB})$ to obtain E_1^h, and finally the combined spin orbit-uniaxial strain splitting E_1^u relative to the CVB is added to give the strained core level referenced to the top of the strain-split valence band E_1^s. The spin orbit-uniaxial strain splitting of the valence bands was calculated from Eqs. (8a)–(8c) of Ref. 5. The parameters used in the calculation are given in Table II, and utilize the experimentally determined values for the deformation potential b. Use of the theoretically calculated deformation potentials listed in Ref. 5 would increase E_1^u by 35 meV and decrease E_2^u by 21 meV. The calculated values are $E_1^u=0.296$ eV and $E_2^u=0.285$ eV. Table III provides a summary of the pa-

TABLE II. Parameter values for calculating E_1^u and E_2^u.

	$10^{-2}\epsilon_{xx}$	$\frac{S_{12}}{S_{11}+S_{12}}$	$10^{-2}\epsilon_{zz}$	Δ_0 (eV)	b (eV)	δE_{001} (eV)	E_1^u (eV)	E_2^u (eV)
Si(100)Ge	+3.962	−0.3857	−3.054	0.044	−2.10	±0.295	0.296	
Ge/(100)Si	−3.811	−0.3754	+2.861	0.282	−2.86	−0.382		0.285

TABLE III. Parameter values in eV for the calculation of valence-band offsets.

Si		Ge	
E_1	99.01	E_2	29.57
E_1^h	99.22	E_2^h	29.56
E_1^u	0.30	E_2^u	0.29
E_1^s	99.53	E_2^s	29.86
$\Delta E_{1,2}$	70.12	$\Delta E_{2,1}$	69.90

rameter values appropriate for evaluation of the band offsets.

Figures 5 and 6 provide schematic band diagrams for Ge on Si(100) and the reverse sequence in terms of our defined parameters. From them one obtains the following relations:

$$\Delta E_v^{2,1}+E_1=E_2^u+E_2^h+\Delta E_{2,1} \quad (3a)$$

and

$$\Delta E_v^{1,2}+E_1^u+E_1^h=E_2+\Delta E_{1,2} \ . \quad (3b)$$

From Table III we obtain $\Delta E_v^{2,1}$[Ge/Si(100)]$=0.74$ eV and $\Delta E_v^{1,2}$[Si/Ge(100)]$=0.17$ eV. For Ge on Si(100) the observed valence-band offset is in reasonable agreement with theory[4] (0.84 eV). The agreement for the reverse growth sequence is somewhat poorer (0.31 eV), although probably not outside the cumulative errors in determining $\Delta E_{1,2}$, E_1, E_2, and the hydrostatic shifts. If we assign an error of 100 meV to the $\Delta E_{1,2}$ measurements and errors of 50 meV each to E_1, E_2, E^u, and E^h, and assume the errors are independent and add in quadrature, then the estimated uncertainty is ± 0.13 eV. The agreement obtained in Ref. 6 with theory was for the case of (Si,Ge) alloys under compression. Similar measurements for alloys under tension have not been reported. The somewhat larger discrepancy between experiment and theory for Si on Ge(100) is not immediately apparent, but based on the Raman measurements, it does not appear to originate in strain relaxation due to misfits.

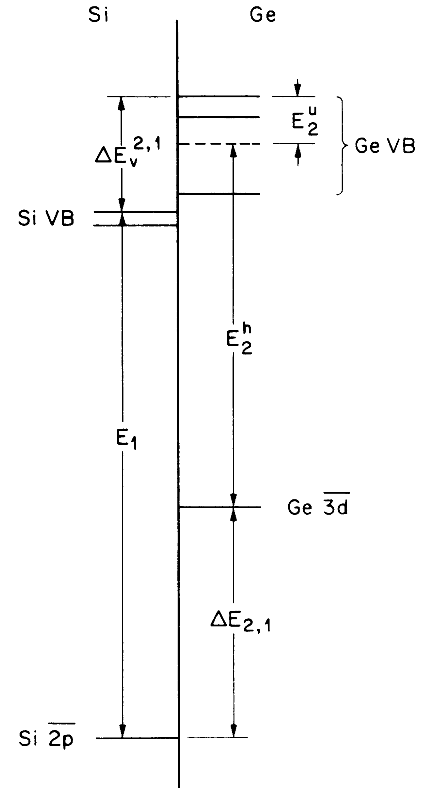

FIG. 6. Schematic energy-band diagram for Si pseudomorphically strained to match the in-plane lattice constant on Ge(100). Parameter values are found in Table III.

IV. CONCLUSION

We have shown, both from direct calculations and measured core-level separations on heterojunction samples, that core levels do not track the valence-band edge in highly strained systems. The magnitude of the strained-induced shift in the core-to-valence-band edge energy can be judged in the Si/Ge system by comparing the values E_1/E_1^2 and E_2/E_2^s in Table III. For this system, these shifts range between 0.3–0.5 eV. In strained heterojunctions, the utilization of photoemission spectroscopy for the evaluation of band offsets must entail either first-principle calculations of relative core–valence-band deformation potentials or reference core levels measured under the appropriate strain conditions. Without supplementing the heterojunction measurements with either of these, the valence-band offsets determined from core-level measurements cannot be expected to correlate with theory in highly strained systems.

ACKNOWLEDGMENT

One of us (M.S.H.) gratefully acknowledges discussion of the core-level calculations with Dr. N. E. Christensen.

[1]S. P. Kowalczyk, R. W. Grant, J. R. Waldrop, and E. A. Kraut, J. Vac. Sci. Technol. B **1**, 684 (1983).

[2]J. R. Waldrop, S. P. Kowalczyk, R. W. Grant, E. A. Kraut, and D. L. Miller, J. Vac. Sci. Technol. **19**, 573 (1981).

[3]J. Tersoff and C. G. Van de Walle, Phys. Rev. Lett. **59**, 946 (1987).

[4]J. Bevk, J. P. Mannaerts, L. C. Feldman, B. A. Davidson, and A. Ourmadz, Appl. Phys. Lett. **49**, 286 (1986).

[5]C. G. Van de Walle and R. M. Martin, Phys. Rev. B **34**, 5621 (1986).

[6]W. X. Ni, J. Knall, and G. V. Hansson, Phys. Rev. B **36**, 7744 (1987).

[7]E. Anastassakis and E. Burstein, J. Phys. Chem. Solids **32**, 563 (1970).
[8]E. Anastassakis and E. Liarokapis, J. Appl. Phys. **62**, 3346 (1987).
[9]F. Cerdeira, D. J. Buchenauer, F. H. Pollak, and M. Cardona, Phys. Rev. B **5**, 580 (1972).
[10]J. Menendez and A. Pinczuk (private communication).
[11]For a general review see C. Colvard, R. Fischer, T. A. Gant, M. V. Klein, R. Merlin, H. Morkoç, and A. C. Gossard, Superlatt. Microstruct. **1**, 81 (1985).
[12]A. Fasolino and E. Molinari, in Proceedings of the Third International Metastable Modulated Semiconductor Structures Conference, Montpellier, 1987 (unpublished).
[13]E.A. Kraut, R. W. Grant, J. R. Waldrop, and S. P. Kowalczyk, Phys. Rev. B **28**, 1965 (1983).
[14]F. J. Himpsel, P. Heimann, T. C. Chiang, and D. E. Eastman, Phys. Rev. Lett. **45**, 1112 (1980).
[15]O. K. Anderson, Phys. Rev. B **12**, 3060 (1975); H. L. Skriver, *The LMTO Method* (Springer-Verlag, New York, 1984).
[16]P. Hohenberg and W. Kohn, Phys. Rev. **136**, B864 (1964); W. Kohn and L. J. Sham, *ibid.* **140**, A1133 (1965). The data for the correlation energy as a function of density are taken from U. von Barth and L. Hedin, J. Phys. C **5**, 1629 (1972).
[17]O. B. Backelet and N. E. Christensen, Phys. Rev. B **31**, 879 (1985).